

Estimating the snow water equivalent on a glacierized high elevation site (Forni Glacier, Italy)

Senese Antonella¹, Maugeri Maurizio¹, Meraldi Eraldo², Verza Gian Pietro³, Azzoni Roberto Sergio¹, Compostella Chiara⁴, Diolaiuti Guglielmina¹

¹ Department of Environmental Science and Policy, Università degli Studi di Milano, Milan, Italy.

² ARPA Lombardia, Centro Nivometeorologico di Bormio, Bormio, Italy.

³ Ev-K2-CNR - Pakistan, Italian K2 Museum Skardu Gilgit Baltistan, Islamabad, Pakistan.

⁴ Department of Earth Sciences, Università degli Studi di Milano, Milan, Italy.

Correspondence to: Antonella Senese (antonella.senese@unimi.it)

Abstract.

We present and compare 11 years of snow data (snow depth and snow water equivalent, *SWE*) measured by an Automatic Weather Station corroborated by data resulting from field campaigns on the Forni Glacier in Italy. The aim of the analyses is to estimate the *SWE* of new snowfall and the annual peak of *SWE* based on the average density of the new snow at the site (corresponding to the snowfall during the standard observation period of 24 hours) and automated snow depth measurements. The results indicate that the daily SR50 sonic ranger measures and the available snow pit data can be used to estimate the mean new snow density value at the site, with an error of $\pm 6 \text{ kg m}^{-3}$. Once the new snow density is known, the sonic ranger allows deriving *SWE* values with a RMSE of 45 mm water equivalent (if compared with snow pillow measurements), that turns out to be about 8% of yearly average total *SWE*. Therefore, the methodology we present is interesting for remote locations such as glaciers or high alpine regions, as it allows estimating total snow water equivalent (*SWE*) using a relatively inexpensive, low power, low maintenance, and reliable instrument such as the sonic ranger.

Keywords: Snow depth; Snow water equivalent (*SWE*); SPICE (Solid Precipitation Intercomparison Experiment) project; Forni Glacier.

1. Introduction and scientific background

The study of the spatial and temporal variability of water resources deriving from snow melt (i.e. Snow Water Equivalent, *SWE*) is very important for estimating the water balance at the catchment scale. In particular, many areas depend on this freshwater reservoir for civil use, irrigation and hydropower, thus making it necessary to have an accurate and updated evaluation of *SWE* magnitude and variability. In addition, a correct *SWE* assessment also supports early strategies for managing and preventing hydro-meteorological risks (e.g. flood forecasting, avalanche forecasting). Moreover, new snow-

37 density evaluation is important for snowfall forecasting based on orographic precipitation models (Judson and Doesken,
38 2000; Roebber et al., 2003), estimation of avalanche hazards (Perla, 1970; LaChapelle, 1980; Ferguson et al., 1990;
39 McClung and Schaerer, 1993), snowdrift forecasting, as an input parameter in the snow accumulation algorithm (Super and
40 Holroyd, 1997), and general snow science research.

41 In high mountain areas, however, often only snowfall measures are available: a correct evaluation of new snow density
42 ($\rho_{new\ snow}$) is therefore needed to calculate the *SWE*. Since new snow density is site specific and depends on atmospheric and
43 surface conditions, the main aim of this study is to investigate the magnitude and rates of variations in $\rho_{new\ snow}$ and to
44 understand how an incorrect assessment of this variable may affect the estimation of the *SWE*. This was possible by means
45 of systematic manual and automatic measurements carried out at the surface of the Forni Glacier (Stelvio Park, Italian Alps,
46 Fig. 1a and b). Since 2005, an Automatic Weather Station (AWS1 Forni) has been acquiring snow data at the glacier
47 surface, in addition to snow pit measurements of snow depth and *SWE* carried out by expert personnel (Citterio et al., 2007;
48 Senese et al., 2012a; 2012b; 2014). The snow data thus acquired refer to snowfall or new snow (i.e. depth of freshly fallen
49 snow deposited over a standard observation period, generally 24 hours, see WMO, 2008; Fierz et al., 2009) and to snow
50 depth (i.e. the total depth of snow on the ground at the time of observation, see WMO, 2008).

51 In general, precipitation can be measured mechanically, optically, by capacitive sensing and by radar. Some examples of
52 available sensors are: the heated tipping bucket rain gauge (as precipitation is collected and melted in the gauge's funnel,
53 water is directed to a tipping bucket mechanism adjusted to tip and dump when a threshold volume of water is collected),
54 the heated weighing gauge (the weight of water collected is measured as a function of time and converted to rainfall depth),
55 the disdrometer (measuring the drop size distribution and the velocity of falling hydrometeors). For catchment type
56 precipitation sensors, the catch efficiency of solid precipitation needs to be considered for the correct measurement of new
57 snow. For the Solid Precipitation Intercomparison Experiment (1989-1993), the International Organizing Committee
58 designated the Double Fence Intercomparison Reference (DFIR) as the reference for intercomparison (WMO/TD-872/1998,
59 section 2.2.2). Even if all these methods mentioned provide accurate measurements, it is very difficult to utilize some of
60 them in remote areas like a glacier site. For this reason, at the Forni Glacier, snow data have been acquired by means of
61 sonic ranger and snow pillow instrumentations, without wind shielding.

62 For estimating *SWE* only from snow depth measurements, estimating a correct new snow density is crucial. Following
63 Roebber et al. (2003), new snow density is often assumed to conform to the 10-to-1 rule: the snow ratio, defined by the
64 density of water (1000 kg m^{-3}) to the density of new snow (assumed to be 100 kg m^{-3}), is 10:1. As noted by Judson and
65 Doesken (2000), the 10-to-1 rule appears to originate from the results of a nineteenth-century Canadian study. More
66 comprehensive measurements (e.g., Currie, 1947; LaChapelle, 1962; Power et al., 1964; Super and Holroyd, 1997; Judson
67 and Doesken, 2000) have established that this rule is an inadequate characterization of the true range of new snow densities.
68 Indeed, they can vary from 10 kg m^{-3} to approximately 350 kg m^{-3} (Roebber et al., 2003). Bocchiola and Rosso (2007)
69 report a similar range for the Central Italian Alps with values varying from 30 kg m^{-3} to 480 kg m^{-3} , and an average sample
70 value of 123 kg m^{-3} . Usually, the lower bound of new snow density is about 50 kg m^{-3} (Gray, 1979; Anderson and
71 Crawford, 1990). Judson and Doesken (2000) found densities of new snow observed from six sheltered avalanche sites in
72 the Central Rocky Mountains to range from 10 to 257 kg m^{-3} , and average densities at each site based on four years of daily
73 observations to range from 72 to 103 kg m^{-3} . Roebber et al. (2003) found that the 10-to-1 rule may be modified slightly to
74 12 to 1 or 20 to 1, depending on the mean or median climatological value of new snow density at a particular station (e.g.

75 Currie 1947; Super and Holroyd, 1997). Following Pahaut (1975), the new snow density ranges from 20 to 200 kg m⁻³ and
76 increases with wind speed and air temperature. Wetzel and Martin (2001) analyzed all empirical techniques evolved in the
77 absence of explicit snow-density forecasts. As argued in Schultz et al. (2002), however, these techniques might be not fully
78 adequate and the accuracy should be carefully verified for a large variety of events.

79 New snow density is regulated by i) in-cloud processes that affect the shape and size of ice crystal growth, ii) sub-cloud
80 thermodynamic stratification through which the ice crystals fall (since the low-level air temperature and relative humidity
81 regulate the processes of sublimation or melting of a snowflake), and iii) ground-level compaction due to prevailing weather
82 conditions and snowpack metamorphism. Understanding how these processes affect new snow density is difficult because
83 direct observations of cloud microphysical processes, thermodynamic profiles, and surface measurements are often
84 unavailable.

85 Cloud microphysical research indicates that many factors contribute to the final structure of an ice crystal. The shape of the
86 ice crystal is determined by the environment in which the ice crystal grows: pure dendrites have the lowest density (Power
87 et al., 1964), although the variation in the density of dendritic aggregates is large (from approximately 5 to 100 kg m⁻³,
88 Magono and Nakamura, 1965; Passarelli and Srivastava, 1979). Numerous observational studies over decades clearly
89 demonstrate that the density varies inversely with size (Magono and Nakamura, 1965; Holroyd, 1971; Muramoto et al.,
90 1995; Fabry and Szyrmer, 1999; Heymsfield et al., 2004; Brandes et al., 2007). The crystal size is related to the ratio
91 between ice and air (Roebber et al., 2003): large dendritic crystals will occupy much empty air space, whereas smaller
92 crystals will pack together into a denser assemblage. In addition, as an ice crystal falls, it passes through varying
93 thermodynamic and moisture conditions. Then, the ultimate shape and size of crystals depend on factors that affect the
94 growth rate and are a combination of various growth modes (e.g. Pruppacher and Klett, 1997).

95 To contribute to the understanding of all the above topics, in this paper we discuss and compare all the available snow data
96 measured at the Forni Glacier surface in the last decade to: i) suggest the most suitable measurement system for evaluating
97 *SWE* at the glacier surface (i.e. snow pillow, sonic ranger, snow pit or snow weighing tube); ii) assess the capability to
98 obtain *SWE* values from the depth measurements and their accuracies; iii) check the validity of the $\rho_{new\ snow}$ value previously
99 found (i.e. 140 kg m⁻³, see Senese et al., 2014) in order to support *SWE* computation; and iv) evaluate effects and impacts of
100 uncertainties in the $\rho_{new\ snow}$ value in relation to the derived *SWE* amount.

101

102

103 **2. Study area and Forni AWSs**

104 The Forni Glacier (one among the largest glaciers in Italy) is a Site of Community Importance (SCI, code IT2040014)
105 located inside an extensive natural protected area (the Stelvio Park). It is a wide valley glacier (ca. 11.34 km² of area,
106 D'Agata et al., 2014), covering an elevation range from 2600 to 3670 m a.s.l.

107 The first Italian supraglacial station (AWS1 Forni, Fig. 1b) was installed on 26th September 2005 at the lower sector of the
108 eastern tongue of Forni Glacier (Citterio et al., 2007; Senese et al., 2012a, 2012b; 2014; 2016). The WGS84 coordinates of
109 AWS1 Forni were: 46° 23' 56.0" N, 10° 35' 25.2" E, 2631 m a.s.l. (Fig. 1a, yellow triangle). The second station (AWS
110 Forni SPICE, Fig. 1b) was installed on 6th May 2014 close to AWS1 Forni (at a distance of about 17 m). Due to the
111 formation of ring faults, in November 2015 both AWSs were moved to the Forni Glacier central tongue (46°23'42.40"N and
112 10°35'24.20"E at an elevation of 2675 m a.s.l., the red star in Fig. 1a). Ring faults are a series of circular or semicircular

113 fractures with stepwise subsidence (caused by englacial or subglacial meltwater) that could compromise the stability of the
114 stations because they could create voids at the ice-bedrock interface and eventually the collapse of cavity roofs (Azzoni et
115 al., 2017; Fugazza et al., 2017).

116 The main challenges in installing and managing Forni AWSs were due to the fact that the site is located on the surface of an
117 Alpine glacier, not always accessible, especially during wintertime when skis and skins are needed on the steep and narrow
118 path, and avalanches can occur. Moreover, the glacier is a dynamic body (moving up to 20-30 m y⁻¹, Urbini et al., 2017) and
119 its surface also features a well-developed roughness due to ice melting, flowing meltwater, differential ablation and opening
120 crevasses (Diolaiuti and Smiraglia, 2010; Smiraglia and Diolaiuti, 2011). In addition, the power to be supplied to
121 instruments and sensors is only provided by solar panels and lead-gel batteries. A thorough and accurate analysis of
122 instruments and devices (i.e. energy supply required, performance and efficiency operation at low temperatures, noise in
123 measuring due to ice flow, etc.) was required before their installation on the supraglacial AWSs to avoid interruptions in
124 data acquisition and storage.

125 AWS1 Forni is equipped with sensors for measuring air temperature and humidity (a naturally ventilated shielded sensor),
126 wind speed and direction, air pressure, and the four components of the radiation budget (longwave and shortwave, both
127 incoming and outgoing fluxes), liquid precipitation (by means of an unheated precipitation gauge), and snow depth by
128 means of the Campbell SR50 sonic ranger (Table 1, see also Senese et al., 2012a).

129 AWS Forni SPICE is equipped with a snow pillow (Park Mechanical steel snow pillow, 150 x 120 x 1.5 cm) and a
130 barometer (STS ATM.1ST) for measuring the snow water equivalent (Table 1, Beaumont, 1965). The measured air pressure
131 permits calibration of the output values recorded by the snow pillow. The snow pillow pressure gauge is a device similar to
132 a large air or water mattress filled with antifreeze. As snow is deposited on this gauge, the pressure increase is related to the
133 accumulating mass and thus to *SWE*. On the mast, an automated camera was installed to photograph the four graduated
134 stakes located at the corners of the snow pillow (Fig. 1b) in order to observe the snow depth. When the snow pillow was
135 installed at AWS Forni SPICE, a second sonic ranger (Sommer USH8) was installed at AWS1 Forni.

136 The whole systems of both AWS1 Forni and AWS Forni SPICE are supported by four-leg stainless steel masts (5 m and 6
137 m high, respectively) standing on the ice surface. In this way, the AWSs stand freely on the ice, and move together with the
138 melting surface during summer (with a mean ice thickness variation of about 4 m per year).

139 The automated instruments are sampled every 60 seconds. The SR50 sonic ranger, wind sensor and barometer samples are
140 averaged every 60 minutes. The air temperature, relative humidity, solar and infrared radiation, and liquid precipitation
141 sample are averaged every 30 minutes. The USH8 sonic ranger and snow pillow sample are averaged every 10 minutes. All
142 data are recorded in a flash memory card, including the basic distribution parameters (minimum, mean, maximum, and
143 standard deviation values).

144 The long sequence of meteorological and glaciological data permitted the introduction of the AWS1 Forni into the SPICE
145 (Solid Precipitation Intercomparison Experiment) project managed and promoted by the WMO (World Meteorological
146 Organization) (Nitu et al., 2012) and the CryoNet project (Global Cryosphere Watch's core project, promoted by the WMO)
147 (Key et al., 2015).

148
149
150

151 3. Data and methods

152 Snow data at the Forni Glacier have been acquired by means of i) a Campbell SR50 sonic ranger from October 2005 (snow
153 depth data), ii) manual snow pits from January 2006 (snow depth and *SWE* data), iii) a Sommer USH8 sonic ranger from
154 May 2014 (snow depth data), iv) a Park Mechanical SS-6048 snow pillow from May 2014 (*SWE* data), v) a manual snow
155 weighing tube (Enel-Valtecne ©) from May 2014 (snow depth and *SWE* data). These measurements were made at the two
156 automatic weather stations (AWSs): AWS1 Forni and AWS Forni SPICE.

157 Comparing the datasets from the Campbell and Sommer sensors, a very good agreement is found ($r = 0.93$). This means that
158 both sensors have worked correctly. In addition, from 2015 onwards, the double snow depth datasets could mean better data
159 for the *SWE* estimate.

160 In addition to the measurements recorded by the AWSs, since winter 2005-2006, personnel from the Centro Nivo-
161 Meteorologico (namely CNM Bormio-ARPA Lombardia) of the Lombardy Regional Agency for the Environment have
162 periodically used snow pits (performed according to the AINEVA protocol, see also Senese et al., 2014) in order to estimate
163 snow depth and *SWE* (in mm water equivalent, w.e.). In particular, for each snow pit j , the thickness (h_{ij}) and the density
164 (ρ_{ij}) of each snow layer (i) are measured for determining its snow water equivalent, and then the total $SWE_{snow-pit-j}$ of the
165 whole snow cover (n layers) is obtained:

$$166 SWE_{snow-pit-j} = \sum_{i=1}^n h_{ij} \cdot \frac{\rho_{ij}}{\rho_{water}} \quad (1)$$

167 where ρ_{water} is water density. As noted in a previous study (Senese et al., 2014), the date when the snow pit is dug is very
168 important for not underestimating the actual accumulation. For this reason, we considered only the snow pits excavated
169 before the beginning of snow ablation. In fact, whenever ablation occurs, successive *SWE* values derived from snow pits
170 show a decreasing trend (i.e., they are affected by mass losses).

171 The snow pit *SWE* data were then used, together with the corresponding total new snow derived from sonic ranger readings,
172 to estimate the site average $\rho_{new\ snow}$, in order to update the value of 140 kg m^{-3} that was found in a previous study of data of
173 the same site covering the period 2005-2009 (Senese et al., 2012a). We need to update our figures for $\rho_{new\ snow}$ as this is the
174 key variable for estimating *SWE* from the sonic ranger's new snow data. Specifically, for each snow pit j , the corresponding
175 total new snow was first determined by:

$$176 \Delta h_{snow-pit-j} = \sum_{t=1}^m (\Delta h_{tj}) \quad (2)$$

177 where m is the total number of days with snowfall in the period corresponding to snow pit j and Δh_{tj} corresponds to the
178 depth of new snow on day t . Indeed, the new snow is defined as the depth of freshly fallen snow deposited over a standard
179 observation period, generally 24 hours (see WMO, 2008; Fierz et al., 2009). In particular, we considered the hourly snow
180 depth values recorded by the sonic ranger in a day and we calculated the difference between the last and the first reading.
181 Whenever this difference is positive (at least 1 cm), it corresponds to a new snowfall. All data are subject to a strict quality
182 control to avoid under- or over-measurements, to remove outliers and nonsense values, and to filter possible noises.
183 $\sum_{t=1}^m (\Delta h_{tj})$ is therefore the total new snow measured by the Campbell SR50 from the beginning of the accumulation period
184 to the date of the snow pit survey. Obviously, this value is higher than the snow depth recorded by the sonic ranger when the
185 snow pit is dug due to settling.

186 The average site $\rho_{new\ snow}$ was then determined as:

$$187 \rho_{new\ snow} = \frac{\sum_{j=1}^k SWE_{snow-pit-j}}{\sum_{j=1}^k (\Delta h_{snow-pit-j})} \quad (3)$$

188 where j identifies a given snow pit and the corresponding total new snow and the sum extends over all k available snow pits.
189 Instead of a mere average of $\rho_{new\ snow}$ values obtained from individual snow pit surveys, this relation gives more weight to
190 snow pits with a higher $SWE_{snow-pit}$ amount.

191 The SWE_{SR} (from sonic ranger data) of each day (t) was then estimated by:

$$192 \quad SWE_{SR-t} = \begin{cases} \Delta h_t \frac{\rho_{new\ snow}}{\rho_{water}} & \text{if } \Delta h_t \geq 1 \text{ cm} \\ 0 & \text{if } \Delta h_t < 1 \text{ cm} \end{cases} \quad (4)$$

193

194

195 4. Results

196 Figure 2 represents the 11-year dataset of snow depth measured by the SR50 sonic ranger from 2005 to 2016. The last data
197 (after October 2015) were recorded in a different site than the previous one because of the AWS's relocation in November
198 2015. The distance between the two sites is about 500 m, the difference in elevation is only 44 m and the aspect is very
199 similar, so we do not expect a noticeable impact of the site change on snow depth.

200 A large inter-annual variability is seen, with a peak of 280 cm (on 2nd May 2008). In general, the maximum snow depth
201 exceeds 200 cm, except in the period 2006-2007, which is characterized by the lowest maximum value (134 cm on 26th
202 March 2007). These values are in agreement with findings over the Italian Alps in the period 1960–2009. In fact, Valt and
203 Cianfarra (2010) reported a mean snow depth of 233 cm (from 199 to 280 cm) for the stations above 1500 m a.s.l. The snow
204 accumulation period generally starts between the end of September and the beginning of October. The snow appears to be
205 completely melted between the second half of June and the beginning of July (Fig. 2).

206 Because of the incomplete dataset from the Sommer USH8 sonic ranger, only the data from the Campbell SR50 sensor are
207 considered for analysis.

208 The updated value of $\rho_{new\ snow}$ is 149 kg m^{-3} , which is similar to findings considering the 2005-2009 dataset (equal to 140 kg
209 m^{-3} , (Senese et al., 2012a). Figure 3 reports the cumulative SWE_{SR} values (i.e. applying Eq. 4) and the ones obtained using
210 snow pit techniques ($SWE_{snow-pit}$) from 2005 to 2016. As found in previous studies (Senese et al., 2012a, 2014), there is a
211 rather good agreement (RMSE = 58 mm w.e. with a mean $SWE_{snow-pit}$ value of 609 mm w.e.) between the two datasets (i.e.
212 measured $SWE_{snow-pit}$ and derived SWE_{SR}). Whenever sonic ranger data are not available for a long period, the derived total
213 SWE value appears to be incorrect. In particular, in addition to the length of missing dataset, the period of the year with
214 missing data influences the magnitude of the actual accumulation underestimation. During the snow accumulation period
215 2010-2011, the data gap from 15 December 2010 to 12 February 2011 (total of 60 days) produces an underestimation of 124
216 mm w.e. corresponding to 16% of the measured value (on 25th April 2011 $SWE_{SR} = 646 \text{ mm w.e.}$ and $SWE_{snow-pit} = 770 \text{ mm}$
217 w.e. , Fig. 3). During the hydrological years 2011-2012 and 2012-2013, there were some problems with sonic ranger data
218 acquisition thus making it impossible to accumulate these data from 31st January 2012 to 25th April 2013. In these cases,
219 there are noticeable differences between the two datasets: on 1st May 2012 $SWE_{snow-pit} = 615 \text{ mm w.e.}$ and $SWE_{SR} = 254 \text{ mm}$
220 w.e. , and on 25th April 2013 $SWE_{snow-pit} = 778 \text{ mm w.e.}$ and $SWE_{SR} = 327 \text{ mm w.e.}$, with an underestimation of 59% and
221 58%, respectively (Fig. 3).

222 Figure 4 reports the comparison between the SWE_{SR} values and the ones obtained using the snow pillow (2014-2016 period).
223 Apart from a first period without or with a very thin cover of snow, the SWE_{SR} curve follows the curve of SWE measured by
224 the snow pillow (Fig. 4), thus suggesting that our approach seems to give reasonable results. In order to better assess the

225 reliability of our derived SWE_{SR} values, a scatter plot of measured (by means of snow pillow, snow weighing tube and snow
226 pit) versus derived SWE data is shown (Fig. 5). The chosen period is the snow accumulation time frame during 2014-2015
227 and 2015-2016: from November 2014 to March 2015 and from February 2016 to May 2016 (i.e. the snow accumulation
228 period, excluding the initial period in which the snow pillow seems to have significant measuring problems). There is a
229 general underestimation of SWE_{SR} compared to the snow pillow values, considering the 2014-2015 data, though the
230 agreement strengthens in the 2015-2016 dataset (Fig. 5): 54 mm w.e. and 29 mm w.e. of RMSE regarding 2014-2015 and
231 2015-2016, respectively. Considering the whole dataset, the RMSE is 45 mm w.e., that turns out to be about 8% of yearly
232 average total SWE measured by the snow pillow. If compared with the snow pit, the difference is 35 mm w.e. (about 6% of
233 the measured value). Nevertheless, numerous measurements made using the snow weighing tube (Enel-Valtecne ©) around
234 the AWSs on 20th February 2015, showed wide variations of snow depth over the area (mean value of 165 cm and standard
235 deviation of 29 cm) even if the snow surface seemed to be homogenous. This was mainly due to the roughness of the glacier
236 ice surface. Indeed, on 20th February 2015 the snow pillow recorded a SWE value of 493 mm w.e., while from the snow pit
237 the SWE was equal to 555 mm w.e., and from the snow weighing tube the SWE ranged from 410 to 552 mm w.e. (Fig. 5),
238 even if all measurements were performed very close to each other.

239

240 5. Discussion

241 5.1 Possible errors related to the methodology

242 Defining a correct algorithm for modeling SWE data is very important for evaluating the water resources deriving from
243 snow melt. The approach applied to derive SWE_{SR} is highly sensitive to the value used for the new snow density, which can
244 vary substantially depending on both atmospheric and surface conditions. In this way, the error in individual snowfall events
245 could be quite large. Moreover, the technique depends on determining snowfall events, which are estimated from changes in
246 snow depth, and the subsequent calculation and accumulation of SWE_{SR} from those events. Therefore, missed events due to
247 gaps in snow depth data could invalidate the calculation of peak SWE_{SR} . For these reasons, we focused our analyses on
248 understanding how an incorrect assessment of $\rho_{new\ snow}$ or a gap in snow depth data may affect the estimation of the SWE .
249 First, we evaluated the $\rho_{new\ snow}$ estimate (applying Eq. 3, found to be equal to 149 kg m⁻³ considering the 2005-2015
250 dataset), by means of the leave-one-out cross-validation technique (LOOCV, a particular case of leave-p-out cross-
251 validation with $p = 1$), to ensure independence between the data we use to estimate $\rho_{new\ snow}$ and the data we use to assess the
252 corresponding estimation error. In this kind of cross-validation, the number of “folds” (repetitions of the cross-validation
253 process) equals the number of observations in the dataset. Specifically, we applied Eq. 3 once for each snow pit (j), using all
254 other snow pits in the calculation ($LOOCV\ \rho_{new\ snow}$) and using the selected snow pit as a single-item test ($\rho_{new\ snow}$ from snow
255 pit j). In this way, we avoid dependence between the calibration and validation datasets in assessing the new snow density.
256 The results are shown in Table 2. Analysis shows that the standard deviation of the differences between the $LOOCV\ \rho_{new\ snow}$
257 values and the corresponding single-item test values ($\rho_{new\ snow}$ from snow pit j) is 18 kg m⁻³. The error of the average value of
258 $\rho_{new\ snow}$ can therefore be estimated dividing this standard deviation by the square root of the number of the considered snow
259 pits. It turns out to be 6 kg m⁻³. The new and the old estimates (149 and 140 kg m⁻³, respectively) therefore do not have a
260 statistically significant difference. The individual snow accumulation periods instead have naturally a higher error and the
261 single snow pit estimates for $\rho_{new\ snow}$ range from 128 to 178 kg m⁻³. In addition, we attempted to extend this analysis
262 considering each single snow layer (h_{ij}) instead of each snow pit j . In particular, we tried to associate to each snow pit layer

263 the corresponding new snow measured by the sonic ranger (Citterio et al., 2007). However, this approach turned out to be
264 too subjective to contribute more quantitative information about the real representativeness of the $\rho_{new\ snow}$ value we found.
265 Moreover, we investigated the *SWE* sensitivity to changes in $\rho_{new\ snow}$. In particular, we calculated *SWE*_{SR} using different
266 values of new snow density ranging from 100 to 200 kg m⁻³ at 25 kg m⁻³ intervals (Fig. 6). An increase/decrease of the
267 density by 25 kg m⁻³ causes a mean variation in *SWE*_{SR} of ±106 mm w.e. for each hydrological year (corresponding to about
268 17% of the mean total cumulative *SWE* considering all hydrological years), ranging from ±43 mm w.e. to ±144 mm w.e. A
269 reliable estimation of $\rho_{new\ snow}$ is therefore a key issue.

270 In addition to an accurate definition of new snow density, an uninterrupted dataset of snow depth is also necessary in order
271 to derive correct *SWE*_{SR} values. This can be deduced also observing the large deviations between the *SWE* values
272 (independent of the chosen snow density) by the SR50 and the snow pit measurements in the years 2010, 2011, 2012 and
273 2013. It is therefore necessary to put in place all the available information to reduce the occurrence of data gaps to a
274 minimum. The introduction of the second sonic ranger (Sommer USH8) at the end of the 2013-2014 snow season was an
275 attempt to reduce the impact of this problem. This second sonic ranger, however, was still in the process of testing in the last
276 years of the period investigated within this paper. We are confident that in the years to come it can help reduce the problem
277 of missing data. Indeed, daily variations in snow depth measured by one sensor could be used to fill the data gap of the other
278 one. Multiple sensors for fail-safe data collection are indeed highly recommended. In addition, the wooden four stakes
279 installed at the corners of the snow pillow at the beginning of the 2014-2015 snow season were another idea for collecting
280 more data. Unfortunately, they were broken almost immediately after the beginning of the snow accumulation period. They
281 can be another way to deal with the problem of missing data, provided we figure out how to avoid breakage during the
282 winter season. Probably the choice of a more robust and white material (such as insulated white steel) could overcome this
283 issue.

284 It is also important to stress that potential errors in individual snowfall events could affect peak *SWE*_{SR} estimation. A large
285 snowfall event with a considerable deviation from the mean new snow density will result in large errors (e.g. a heavy wet
286 snowfall). These events are rather rare at the Forni site: only 3 days in the 11-year period covered by the data recorded more
287 than 40 cm of new snow (the number of days decreases to 1 if the threshold increases to 50 cm). Therefore, even if the
288 proposed technique can be susceptible to these errors, high precipitation amounts are infrequent, reducing the likelihood of
289 this happening at the Forni site. Without knowing the true density of the new snow during these big events, it's difficult to
290 know their impact on the *SWE* estimate. However, assuming that the new snow density could be increased from 149 kg m⁻³
291 to 200 kg m⁻³, the difference in *SWE* for a large event (e.g. 30 cm) is 15 mm w.e. (45 mm w.e. with 149 kg m⁻³ and 60 mm
292 w.e. with 200 kg m⁻³).

293 Our new snow data could be affected by settling, sublimation, snow transported by wind, and rainfall. As far as settling is
294 concerned, $\Delta h_{snow-pit-j}$ from Eq. 2 would indeed be higher if Δh_{tj} values were calculated considering an interval shorter
295 than 24 hours. However, this would not be possible because on the one hand, the sonic ranger data's margin of error is too
296 high to consider hourly resolution, and on the other hand, new snow is defined by the WMO within the context of a 24-hour
297 period. Settling processes can concern also the snow pack under the new snow layer. This process can affect our daily
298 differences mainly with snowfall lasting for several days. In this case, the measured daily positive snow depth differences
299 could be smaller than the real depth of the new snow, with the consequence of overestimating new snow density. However,
300 the obtained mean new snow density is not so higher than the general values found in literature. In addition, the comparison

301 with snow pillow dataset seems supporting our methodology. On the other hand, if many days pass between one snowfall
302 and the following one, the settlement of the snow pack under the new snow layer is less likely to affect the measured
303 differences in snow depth and this seems to be the case of the Forni Glacier site as snow days are only 9% of the snow
304 season days. Regarding the transport by wind, the effect that is potentially more relevant is new snow that is recorded by the
305 sonic ranger but then blown away in the following days. It is therefore considered in $\Delta h_{snow-pit-j}$ but not in
306 $SWE_{snow-pit-j}$, thus causing an underestimation of $\rho_{new\ snow}$ (see Eq. 3). The snow transported to the measuring site can
307 also influence $\rho_{new\ snow}$ even if in this case the effect is less important as it measured both by the sonic ranger and by the
308 snow pit. Here, the problem may be an overestimation of $\rho_{new\ snow}$ as snow transported by wind usually has a higher
309 density than new snow. We considered the problem of the effect of wind on snow cover when we selected the station site on
310 the glacier. Even though sites not affected by wind transport simply do not exist, we are confident that the site we selected
311 has a position that can reasonably minimize this issue. Moreover, sublimation processes would have an effect that is similar
312 to those produced by new snow that is recorded by the sonic ranger but then blown away in the following days. In any case,
313 the value we found for the site average new snow density (i.e. 149 kg m^{-3}) does not seem to suggest an underestimated
314 value. Finally, another possible source of error in estimating new snow density and in deriving the daily SWE is represented
315 by rainfall events. In fact, one of the effects is an enhanced snow melt and then a decrease in snow depth, as rain water has a
316 higher temperature than the snow. Therefore, especially at the beginning of the snow accumulation season, we could detect
317 a snowfall (analyzing snow depth data) but whenever it was followed by a rainfall, the new fallen snow could partially or
318 completely melt, thus remaining undetected when measured at the end of the accumulation season using snow pit
319 techniques. This is therefore another potential error that, besides the ones previously considered, could lead to
320 underestimation of the $\rho_{new\ snow}$ value, even if, as already mentioned, the value of 149 kg m^{-3} does not seem to suggest this.
321 On the other hand, rain can also increase the SWE measured using the snow pit techniques without giving a corresponding
322 signal in the sonic ranger measurements of snow depth whenever limited amounts of rain fall over cold snow. Anyway, rain
323 events are extremely rare during the snow accumulation period, so the errors associated with rain are minimal.

324

325 5.2 Possible errors related to the instrumentation

326 In regards to the instrumentation, we found some issues related to the derived snow information. Focusing on the beginning
327 of the snow accumulation period, it appears that neither system of measurement (i.e. sonic ranger and snow pillow) is able
328 to correctly detect the first snowfall events. With the sonic ranger, the surface roughness of the glacier ice makes it
329 impossible to distinguish a few centimeters of freshly fallen snow. In fact, the surface heterogeneity (i.e. bare ice, ponds of
330 different size and depth, presence of dust and fine or coarse debris that can be scattered over the surface or aggregated)
331 translates into a differential ablation, due to different values of albedo and heat transfer. These conditions cause differences
332 in surface elevation of up to tens of centimeters and affects the angular distribution of reflected ultrasound. At 3 m of height,
333 the diameter of the measuring field is 1.17 m for the SR50. For these reasons, the sonic ranger generally records inconsistent
334 distances between ice surface and sensor, generally much smaller than the values of the previous and subsequent readings.

335 This issue does not occur with thick snow cover as the snow roughness is very minor compared to that of ice.

336 Regarding the snow pillow methodology, analyzing the 2014-2015 and 2015-2016 data, it seems to work correctly only
337 with a snow cover thicker than 50 cm (Fig. 4). In fact, with null or very low snow depth, SWE values are incorrectly
338 recorded. The results from the snow pillow are difficult to explain as this sensor has been working for only two winter

339 seasons and we are still in the process of testing it. Analyzing data from the years to come will allow a more robust
340 interpretation. However, we have searched for a possible explanation of this problem and this error could be due to the
341 configuration of the snow pillow. Moreover, some of the under-measurement or over-measurement errors can commonly be
342 attributed to differences in the amount of snow settlement over the snow pillow, compared with that over the surrounding
343 ground, or to bridging over the snow pillow with cold conditions during development of the snow cover (Beaumont, 1965).
344 In addition, another major source of *SWE* snow pillow errors is generally due to measuring problems of this device, which is
345 sensitive to the thermal conditions of the sensor, the ground and the snow (Johnson et al., 2015). In fact, according to
346 Johnson and Schaefer (2002) and Johnson (2004) snow pillow under-measurement and over-measurement errors can be
347 related to the amount of heat conduction from the ground into the overlying snow cover, the temperature at the ground/snow
348 interface and the insulating effect of the overlying snow. This particular situation can not be recognized at the Forni Glacier
349 as the surface consists of ice and not of soil . Therefore, in our particular case the initial error could be due to the
350 configuration of the snow pillow.

351 In order to assess the correct beginning of the snow accumulation period and overcome the instrument issues, albedo
352 represents a useful tool, as freshly fallen snow and ice are characterized by very different values (e.g. Azzoni et al., 2016).
353 In fact, whenever a snowfall event occurs, albedo immediately rises from about 0.2 to 0.9 (typical values of ice and freshly
354 fallen snow, respectively, Senese et al., 2012a). This is also confirmed by the automated camera's hourly pictures. During
355 the hydrological year 2014-2015, the first snowfall was detected on 22nd October 2014 by analyzing albedo data, and it is
356 verified by pictures taken by the automated camera. Before this date, the sonic ranger did not record a null snow depth,
357 mainly due to the ice roughness; therefore, we had to correct the dataset accordingly.

358 Concerning the *SWE* as determined by the snow weighing tube, this device is pushed vertically into the snow to fill the tube.
359 The tube is then withdrawn from the snow and weighed. Knowing the length of tube filled with snow, the cross-sectional
360 area of the tube and the weight of the snow allows a determination of both the *SWE* and the snow density (Johnson et al.,
361 2015). The measurements carried out around the AWSs on 20th February 2015 showed a great spatial variability in *SWE*
362 (Fig. 5): the standard deviation is 54 mm w.e., corresponding to 12% of the mean value from snow weighing tube
363 measurements. This could explain the differences found analyzing data acquired using the snow pillow techniques,
364 measured by the snow pit, and derived by the sonic ranger. Nevertheless, the *SWE* variability highlighted by the snow
365 weighing tube surveys can be also due to oversampling by this device (Work et al., 1965). Numerous studies have been
366 conducted to verify snow tube accuracy in determining *SWE*. The most recent studies by Sturm et al. (2010) and Dixon and
367 Boon (2012) found that snow tubes could under- or over-measure *SWE* from -9% to +11%. Even if we allow for $\pm 10\%$
368 margin of error in our snow tube measurements, the high *SWE* variability is confirmed.

369 Finally, the last approach for measuring *SWE* is represented by the snow pit. This method (like the snow tube) has the
370 downside that it is labor intensive and it requires expert personnel. Moreover, as discussed in Senese et al. (2014), it is very
371 important to select a correct date for making the snow pit surveys in order to assess the total snow accumulation amount.
372 Generally, 1st April is the date considered the most indicative of the peak cumulative *SWE* in high mountain environments
373 of the midlatitudes, but this day is not always the best one. In fact, Senese et al. (2014) found that using a fixed date for
374 measuring the peak cumulative *SWE* is not the most suitable solution. In particular, they suggest that a correct temperature
375 threshold can help to determine the most appropriate time window of analysis, indicating the starting time of snow melting
376 processes and then the end of the accumulation period. From the Forni Glacier, the application of the $+0.5^{\circ}\text{C}$ daily

377 temperature threshold allows for a consistent quantification of snow ablation while, instead, for detecting the beginning of
378 the snow melting processes, a suitable threshold has proven to be at least -4.6°C . A possible solution to this problem could
379 be to repeat the snow pit surveys over the same period to verify the variability of microscale conditions. This can be useful
380 especially in those remote areas where no snowfall information is available. However, this approach involves too much time
381 and resources and is not always feasible.

382 Even if the generally used sensors (such as the heated tipping bucket rain gauge, the heated weighing gauge, or the
383 disdrometer) provide more accurate measurements, in remote areas like a glacier, it is very difficult to install and maintain
384 them. One of the limitations concerns the power to be supplied to instruments, which can only consist in solar panels and
385 lead-gel batteries. In fact, at the Forni site we had to choose only unheated low-power sensors. The snow pillow turned out
386 to be logistically unsuitable, as it required frequent maintenance. Especially with bare ice or few centimeters of snow cover,
387 the differential ablation causes instability of the snow pillow, mainly due to its size. Therefore, the first test on this sensor
388 seems to indicate that it did not turn out to be appropriate for a glacier surface. We will, however, try to get better results
389 from it in the coming years. The snow pit can represent a useful approach but it requires expert personnel for carrying out
390 the measurements, and the usefulness of the data so-obtained depends on the date for excavating the snow pits. The
391 automated camera provided hourly photos, but for assessing a correct snow depth at least two graduated rods have to be
392 installed close to the automated camera. However, over a glacier surface, glacier dynamics and snow flux can compromise
393 the stability of the rods: in fact, at the AWS Forni SPICE we found them broken after a short while. Finally, the SR50 sonic
394 ranger features the unique problem of the definition of the start of the accumulation period, but this can be overcome using
395 albedo data.

396

397

398 6. Conclusions

399 For the SPICE project, snow measurements at the Forni Glacier (Italian Alps) have been implemented by means of several
400 automatic and manual approaches since 2014. This has allowed an accurate comparison and evaluation of the pros and cons
401 of using the snow pillow, sonic ranger, snow pit, or snow weighing tube, and of estimating *SWE* from snow depth data. We
402 found that the mean new snow density changes based on the considered period was: 140 kg m^{-3} in 2005-2009 (Senese et al.,
403 2014) and 149 kg m^{-3} in 2005-2015. The difference is however not statistically significant. We first evaluated the new snow
404 density estimation by means of LOOCV and we found an error of 6 kg m^{-3} . Then, we benchmarked the derived *SWE*_{SR} data
405 against the information from the snow pillow (data which was not used as input in our density estimation), finding a RMSE
406 of 45 mm w.e. (corresponding to 8% of the maximum *SWE* measured by means of the snow pillow). These analyses
407 permitted a correct definition of the reliability of our method in deriving *SWE* from snow depth data. Moreover, in order to
408 define the effects and impacts of an incorrect $\rho_{\text{new snow}}$ value in the derived *SWE* amount, we found that a change in density
409 of $\pm 25\text{ kg m}^{-3}$ causes a mean variation of 17% of the mean total cumulative *SWE* considering all hydrological years. Finally,
410 once $\rho_{\text{new snow}}$ is known, the sonic ranger can be considered a suitable device on a glacier, or in a remote area in general, for
411 recording snowfall events and for measuring snow depth values in order to derive *SWE* values. In fact, the methodology we
412 have presented here can be interesting for other sites as it allows estimating total *SWE* using a relatively inexpensive, low
413 power, low maintenance, and reliable instrument such as the sonic ranger, and it is a good solution for estimating *SWE* at

414 remote locations such as glacier or high alpine regions. In addition, our methodology provided that the mean new snowfall
415 density can be reliably estimated.

416 Although conventional precipitation sensors, such as heating tipping bucket rain gauges, heated weighing gauges or
417 disdrometers, can perhaps provide more accurate estimates of precipitation and *SWE* than the ones installed at the Forni
418 Glacier, they are less than ideal for use in high alpine and glacier sites. The problem is that in remote areas like a glacier at a
419 high alpine site, it is very difficult to install and maintain them. The main constrictions concern i) the power supply to the
420 instruments, which consists in solar panels and lead-gel batteries, and ii) the glacier dynamics, snow flux and differential
421 snow/ice ablation that can compromise the stability of the instrument structure. Therefore, a sonic ranger could represent a
422 useful approach for estimating *SWE*, since it does not require expert personnel, nor does it depend on the date of the survey
423 (as do such manual techniques as snow pits and snow weighing tubes); it is not subject to glacier dynamics, snow flux or
424 differential ablation (as are graduated rods installed close to an automated camera and snow pillows), and it does not
425 required a lot of power (unlike heated tipping bucket rain gauges). The average new snow density must, however, be known
426 either by means of snow pit measurements or by the availability of information from similar sites in the same geographic
427 area.

428

429 **Acknowledgements**

430 The AWS1 Forni was developed under the umbrella of the SHARE (Stations at High Altitude for Research on the
431 Environment) program, managed by the Ev-K2-CNR Association from 2002 to 2014; it was part of the former CEOP
432 network (Coordinated Energy and Water Cycle Observation Project) promoted by the WCRP (World Climate Research
433 Programme) within the framework of the online GEWEX project (Global Energy and Water Cycle Experiment); it was
434 inserted in the SPICE (Solid Precipitation Intercomparison Experiment) project managed and promoted by the WMO
435 (World Meteorological Organization), and in the CryoNet project (core network of Global Cryosphere Watch promoted by
436 the WMO), and it was applied in the ESSEM COST Action ES1404 (a European network for a harmonised monitoring of
437 snow for the benefit of climate change scenarios, hydrology and numerical weather prediction).

438 This research has been carried out under the umbrella of a research project funded by Sanpellegrino Levissima Spa, and
439 young researchers involved in the study were supported by the DARAS (Department of regional affairs, autonomies and
440 sport) of the Presidency of the Council of Ministers of the Italian government through the GlacioVAR project (PI G.
441 Diolaiuti). Moreover, the Stelvio Park - ERSAF kindly supported data analyses and has been hosting the AWS1 Forni and
442 the AWS SPICE at the surface of the Forni Glacier thus making possible the launch of glacier micro-meteorology in Italy.

443

444 **References**

445 Anderson, E.A. and Crawford, N.H.: The synthesis of continuous snowmelt hydrographs on digital computer. Tech. Rep. n.
446 36, Department Of Civil Engineering of the Stanford university, as reported in: Bras, 1990; 1964.

447 Azzoni, R.S., Senese, A., Zerboni, A., Maugeri, M., Smiraglia, C., and Diolaiuti, G.: Estimating ice albedo from fine debris
448 cover quantified by a semi-automatic method: the case study of Forni Glacier, Italian Alps. *The Cryosphere*, 10, 665–
449 679. 2016doi:10.5194/tc-10-665-2016. Available online at [http://www.the-cryosphere.net/10/665/2016/tc-10-665-](http://www.the-cryosphere.net/10/665/2016/tc-10-665-2016.pdf)
450 2016.pdf

451 Azzoni, R.S., Fugazza, D., Zennaro, M., Zucali, M., D'Agata, C., Maragno, M., Smiraglia, C., and Diolaiuti, G.A.: Recent
452 structural evolution of Forni Glacier tongue (Ortles-Cevedale Group, Central Italian Alps). *Journal of Maps* 13(2) 870-
453 878, 2017.

454 Beaumont, R.T.: Mt. Hood pressure pillow snow gauge, *J. Appl. Meteorol.*, 4, 626–631, 1965.

455 Bocchiola, D. and Rosso, R.: The distribution of daily snow water equivalent in the central Italian Alps. *Advances in Water*
456 *Resources* 30 (2007) 135–147, 2007.

457 Brandes, E.A., Ikeda, K., Zhang, G., Schonhuber, M., and Rasmussen, R.M.: A statistical and physical description of
458 hydrometeor distributions in Colorado snowstorms using a video disdrometer. *J. Appl. Meteor. Climatol.*, 46, 634–650,
459 2007.

460 Citterio, M., Diolaiuti, G., Smiraglia, C., Verza, G., and Meraldi, E.: Initial results from the automatic weather station
461 (AWS) on the ablation tongue of Forni Glacier (Upper Valtellina, Italy), *Geogr. Fis. Din. Quat.*, 30, 141-151, 2007.

462 Currie, B. W., 1947: Water content of snow in cold climates. *Bull. Amer. Meteor. Soc.*, 28, 150–151.

463 D'Agata, C., Bocchiola, D., Maragno, D., Smiraglia, C., and Diolaiuti, G.A.: Glacier shrinkage driven by climate change in
464 The Ortles-Cevedale group (Stelvio National Park, Lombardy, Italian Alps) during half a century (1954-2007).
465 *Theoretical Applied Climatology*, April 2014, Volume 116, Issue 1-2, pp 169-190, 2014.
466 <http://link.springer.com/article/10.1007/s00704-013-0938-5>

467 Diolaiuti, G. and Smiraglia, C.: Changing glaciers in a changing climate: how vanishing geomorphosites have been
468 driving deep changes in mountain landscapes and environments, *Geomorphologie*, 2, 131–152, 2010.

469 Dixon, D. and Boon, S.: Comparison of the SnowHydro snow sampler with existing snow tube designs. *Hydrologic*
470 *Processes* 26 (17), 2555-2562, 2012.

471 Fabry, F. and Szyrmer, W.: Modeling of the melting layer. Part II: Electromagnetic. *J. Atmos. Sci.*, 56, 3593–3600, 1999.

472 Ferguson, S. A., Moore, M.B., Marriott, R.T., and Speers-Hayes, P.: Avalanche weather forecasting at the northwest
473 avalanche center, Seattle, WA. *J. Glaciol.*, 36, 57–66, 1990.

474 Fugazza, D., Scaioni, M., Corti, M., D'Agata, C., Azzoni, R.S., Cernuschi, M., Smiraglia, C., and Diolaiuti, G.: Combination
475 of UAV and terrestrial photogrammetry to assess rapid glacier evolution and conditions of glacier hazards. *Nat. Hazards*
476 *Earth Syst. Sci. Discuss.*, <https://doi.org/10.5194/nhess-2017-198>, in review, 2017.

477 Gray, D.M.: Snow accumulation and distribution. In: Colbeck SC, Ray M, eds., *Proceedings: proceedings, modeling of*
478 *snow cover runoff*, Hanover, NH, 3–33, 1979.

479 Heymsfield, A.J., Bansemer, A., Schmitt, C., Twohy, C., and Poellot, M.R.: Effective ice particle densities derived from
480 aircraft data. *J. Atmos. Sci.*, 61, 982–1003, 2004.

481 Holroyd, E.W., III: The meso- and microscale structure of Great Lakes snowstorm bands: A synthesis of ground
482 measurements, radar data, and satellite observations. Ph.D. dissertation, University at Albany, State University of New
483 York, 148 pp, 1971.

484 Johnson, J.B. and Schaefer, G.: The influence of thermal, hydrologic, and snow deformation mechanisms on snow water
485 equivalent pressure sensor accuracy. *Hydrological Processes* 16: 3529–3542, 2002.

486 Johnson, J.B.: A theory of pressure sensor performance in snow. *Hydrological Processes* 18, 53–64, 2004.

487 Johnson, J.B., Gelvin, A.B., Duvoy, P., Schaefer, G.L., Poole, G., and Horton, G.D.: Performance characteristics of a new
488 electronic snow water equivalent sensor in different climates. *Hydrological Processes*, 29(6), 1418-1433, 2015.

489 Judson, A. and Doesken, N.: Density of freshly fallen snow in the central Rocky Mountains. *Bull. Amer. Meteor. Soc.*, 81,
490 1577–1587, 2000.

491 Key, J., Goodison, B., Schöner, W., Godøy, Ø, Ondráš, M. and Snorrason, Á.: A Global Cryosphere Watch, *Arctic*, 68, 48-
492 58, 2015, <http://www.jstor.org/stable/43871386>

493 LaChapelle, E.R.: The density distribution of new snow. Project F, Progress Rep. 2, USDA Forest Service, Wasatch
494 National Forest, Alta Avalanche Study Center, Salt Lake City, UT, 13 pp, 1962.

495 LaChapelle, E.R.: The fundamental process in conventional avalanche forecasting. *J. Glaciol.*, 26, 75–84, 1980.

496 Magono, C. and Nakamura, T.: Aerodynamic studies of falling snow flakes. *J. Meteor. Soc. Japan*, 43, 139–147, 1965.

497 McClung, D.M. and Schaerer, P.A.: The avalanche handbook. Seattle, WA, The Mountaineers, 1993.

498 Muramoto, K.I., Matsuura, K., and Shiina, T.: Measuring the density of snow particles and snowfall rate. *Electron.*
499 *Commun. Japan*, 78, 71–79, 1995.

500 Nitu, R., Rasmussen, R., Baker, B., Lanzinger, E., Joe, P., Yang, D., Smith, C., Roulet, Y., Goodison, B., Liang, H.,
501 Sabatini, F., Kochendorfer, J., Wolff, M., Hendrikx, J., Vuerich, E., Lanza, L., Aulamo, O. and Vuglinsky, V.: WMO
502 intercomparison of instruments and methods for the measurement of solid precipitation and snow on the ground:
503 organization of the experiment, WMO Technical Conference on meteorological and environmental instruments and
504 methods of observations, Brussels, Belgium, [https://www.wmo.int/pages/prog/www/IMOP/publications/IOM-](https://www.wmo.int/pages/prog/www/IMOP/publications/IOM-109_TECO-2012/Session1/O1_01_Nitu_SPICE.pdf)
505 [109_TECO-2012/Session1/O1_01_Nitu_SPICE.pdf](https://www.wmo.int/pages/prog/www/IMOP/publications/IOM-109_TECO-2012/Session1/O1_01_Nitu_SPICE.pdf), 16–18, 2012.

506 Nolin, A.W., Fetterer, F.M., and Scambos, T.A.: Surface roughness characterizations of sea ice and ice sheets: Case studies
507 with MISR data. *IEEE transactions on Geoscience and Remote Sensing*, 40(7), 1605-1615, 2002.

508 Pahaut, E.: Les cristaux de neige et leurs metamorphoses. Monographies de la Meteorologie Nationale, 1975.

509 Passarelli, R.E.Jr. and Srivastava, R.C.: A new aspect of snowflake aggregation theory. *J. Atmos. Sci.*, 36, 484–493, 1979.

510 Perla, R.: On contributory factors in avalanche hazard evaluation. *Can. Geotech. J.*, 7, 414–419, 1970.

511 Power, B.A., Summers, P.W., and d’Avignon, J.: Snow crystal forms and riming effects as related to snowfall density and
512 general storm conditions. *J. Atmos. Sci.*, 21, 300–305, 1964.

513 Pruppacher, H.R. and Klett, J.D.: *Microphysics of Clouds and Precipitation*. 2d ed. Kluwer Academic, 954 pp, 1997.

514 Roebber, P.J., Bruening, S.L., Schultz, D.M., and Cortinas Jr, J.V.: Improving snowfall forecasting by diagnosing snow
515 density. *Weather and Forecasting*, 18(2), 264-287, 2003.

516 Schultz, D.M., Cortinas Jr., J.V., and Doswell III, C.A.: Comments on “An operational ingredients-based methodology for
517 forecasting midlatitude winter season precipitation.” *Wea. Forecasting*, 17, 160–167, 2002.

518 Senese, A., Diolaiuti, G., Mihalcea, C., and Smiraglia, C.: Energy and mass balance of Forni Glacier (Stelvio National Park,
519 Italian Alps) from a 4-year meteorological data record, *Arct. Antarct. Alp. Res.*, 44, 122–134, 2012a.

520 Senese, A., Diolaiuti, G., Verza, G. P., and Smiraglia, C.: Surface energy budget and melt amount for the years 2009 and
521 2010 at the Forni Glacier (Italian Alps, Lombardy), *Geogr. Fis. Din. Quat.*, 35, 69–77, 2012b.

522 Senese, A., Maugeri, M., Vuillermoz, E., Smiraglia, C., and Diolaiuti, G.: Using daily air temperature thresholds to evaluate
523 snow melting occurrence and amount on Alpine glaciers by T-index models: the case study of the Forni Glacier (Italy).
524 *The Cryosphere*, 8, 1921–1933, 2014. www.the-cryosphere.net/8/1921/2014/

525 Senese, A., Maugeri, M., Ferrari, S., Confortola, G., Soncini, A., Bocchiola, D., and Diolaiuti, G.: Modelling shortwave and
526 longwave downward radiation and air temperature driving ablation at the Forni Glacier (Stelvio National Park, Italy).
527 *Geogr. Fis. Dinam. Quat.*, 39 (1), 89-100, 2016. DOI 10.4461/GFDQ. 2016.39.9

528 Super, A.B. and Holroyd III, E.W.: Snow accumulation algorithm for the WSR-88D radar: Second annual report. Bureau
529 Reclamation Tech. Rep. R-97-05, U.S. Dept. of Interior, Denver, CO, 77 pp., 1997. [Available from National Technical
530 Information Service, 5285 Port Royal Rd., Springfield, VA 22161.]

531 Smiraglia, C. and Diolaiuti, G.: Epiglacial morphology. In Singh VP, Haritashya UK, Singh P eds *Encyclopedia of Snow,*
532 *Ice and Glaciers* Springer, Berlin, 2011.

533 Sturm, M., Taras, B., Liston, G.E., Derksen, C., Jones, T., and Lea, J.: Estimating snow water equivalent using snow depth
534 data and climate classes. *Journal of Hydrometeorology* 11: 1380–1394, 2010.

535 Urbini, S., Zirizzotti, A., Baskaradas, J., Tabacco, I.E., Cafarella, L., Senese, A., Smiraglia, C., and Diolaiuti, G.: Airborne
536 Radio Echo Sounding (RES) measures on Alpine Glaciers to evaluate ice thickness and bedrock geometry: preliminary
537 results from pilot tests performed in the Ortles Cevedale Group (Italian Alps). *Annals of Geophysics*, 60(2), 0226, 2017.

538 Valt, M. and Cianfarra, P.: Recent snow cover variability in the Italian Alps. *Cold Regions Science and Technology*, 64,
539 146-157, 2010.

540 Wetzel, S.W. and Martin, J.E.: An operational ingredients-based methodology for forecasting midlatitude winter season
541 precipitation. *Wea. Forecasting*, 16, 156–167, 2001.

542 Work, R.A., Stockwell, H.J., Freeman, T.G., and Beaumont, R.T.: Accuracy of field snow surveys, Tech. Rep. 163, U.S.
543 Army Cold Reg. Res. and Eng. Lab., Hanover, N. H., 1965.

544 WMO Solid Precipitation Measurement Intercomparison: Final report. WMO/TD - No. 872. Instruments and observing
545 methods, Report No. 67, 202 pp, 1998.

546 WMO: Guide to Meteorological Instruments and Methods of Observation – WMO-No. 8 - Seventh edition, 2008.
547

548 Table 1: Instrumentation at the Forni Glacier with instrument name, measured parameter, manufacturer, and starting date.

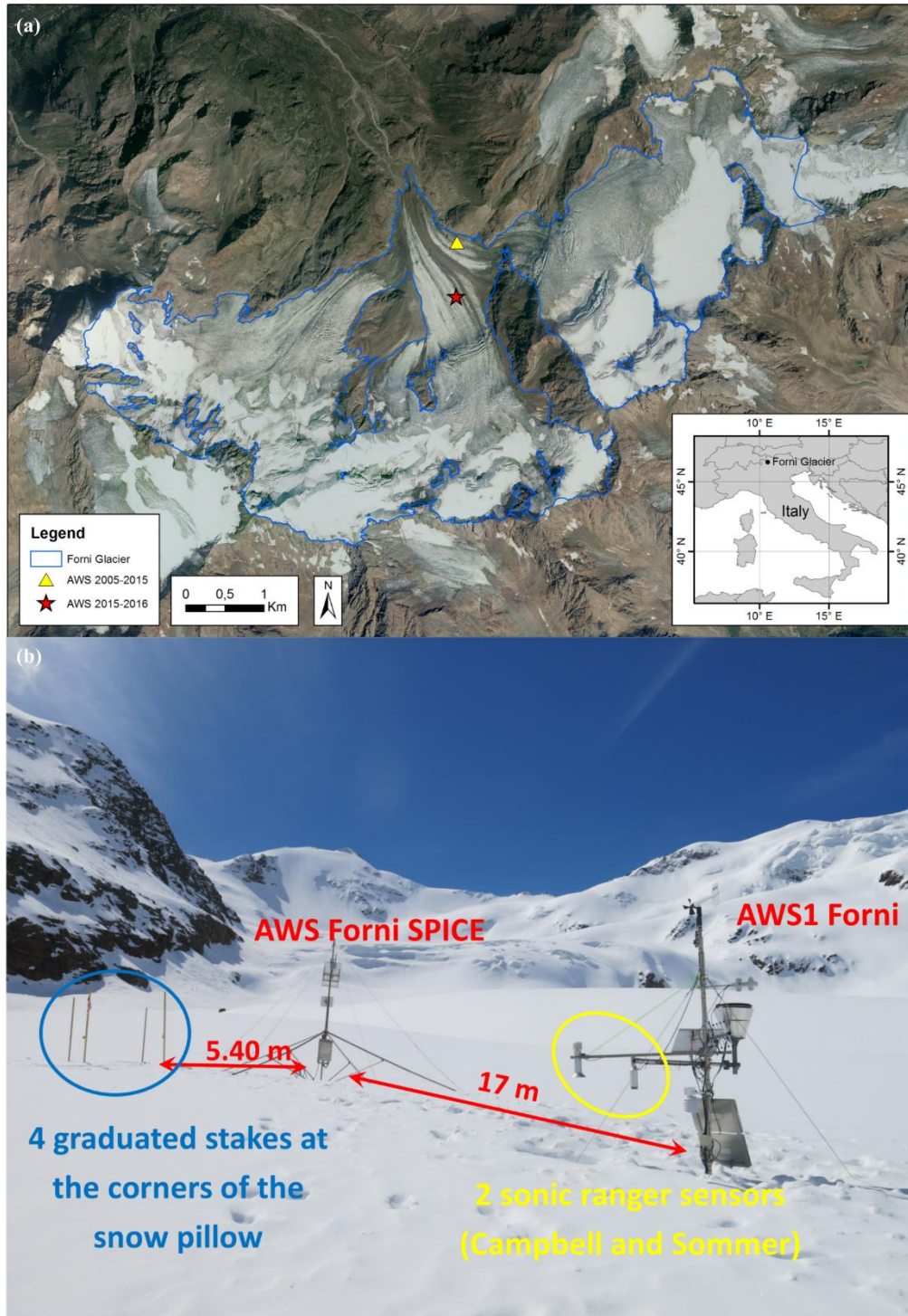
Instrument name	Parameter	Manufacturer	Date
Babuc ABC	Data logger	LSI LASTEM	Sept. 2005
CR200	Data logger	Campbell	May 2014
CR1000	Data logger	Campbell	May 2014
Sonic ranger SR50	Snow depth	Campbell	Sept. 2005
Sonic ranger USH8	Snow depth	Sommer	May 2014
Snow pillow	SWE	Park Mechanical Inc.	May 2014
Thermo-hygrometer	Air temperature and humidity	LSI LASTEM	Sept. 2005
Barometer	Atmospheric pressure	LSI LASTEM	Sept. 2005
Net Radiometer CNR1	Short and long wave radiation fluxes	Kipp & Zonen	Sept. 2005
Pluviometer unheated	Liquid precipitation	LSI LASTEM	Sept. 2005
Anemometer 05103V	Wind speed and direction	Young	Sept. 2005

549

550 Table 2: The leave-one-out cross-validation (LOOCV). For each survey, we reported the SWE values measured by means of
 551 the snow pit ($SWE_{snow-pit}$), the values of the new snow density applying the Eq. 3 ($\rho_{new\ snow}$ from snow pit j), and the new
 552 snow density obtained applying the LOOCV method ($LOOCV\ \rho_{new\ snow}$).

Date of survey	$SWE_{snow-pit}$ (mm w.e.)	$\rho_{new\ snow}$ from snow pit j (kg m⁻³)	LOOCV $\rho_{new\ snow}$ (kg m⁻³)
24/01/06	337	147	150
02/03/06	430	128	153
30/03/06	619	147	150
07/05/08	690	135	152
21/02/09	650	143	151
27/03/10	640	156	149
25/04/11	770	178	147
20/02/15	555	159	149
MEAN		149	150

553



554

555

556

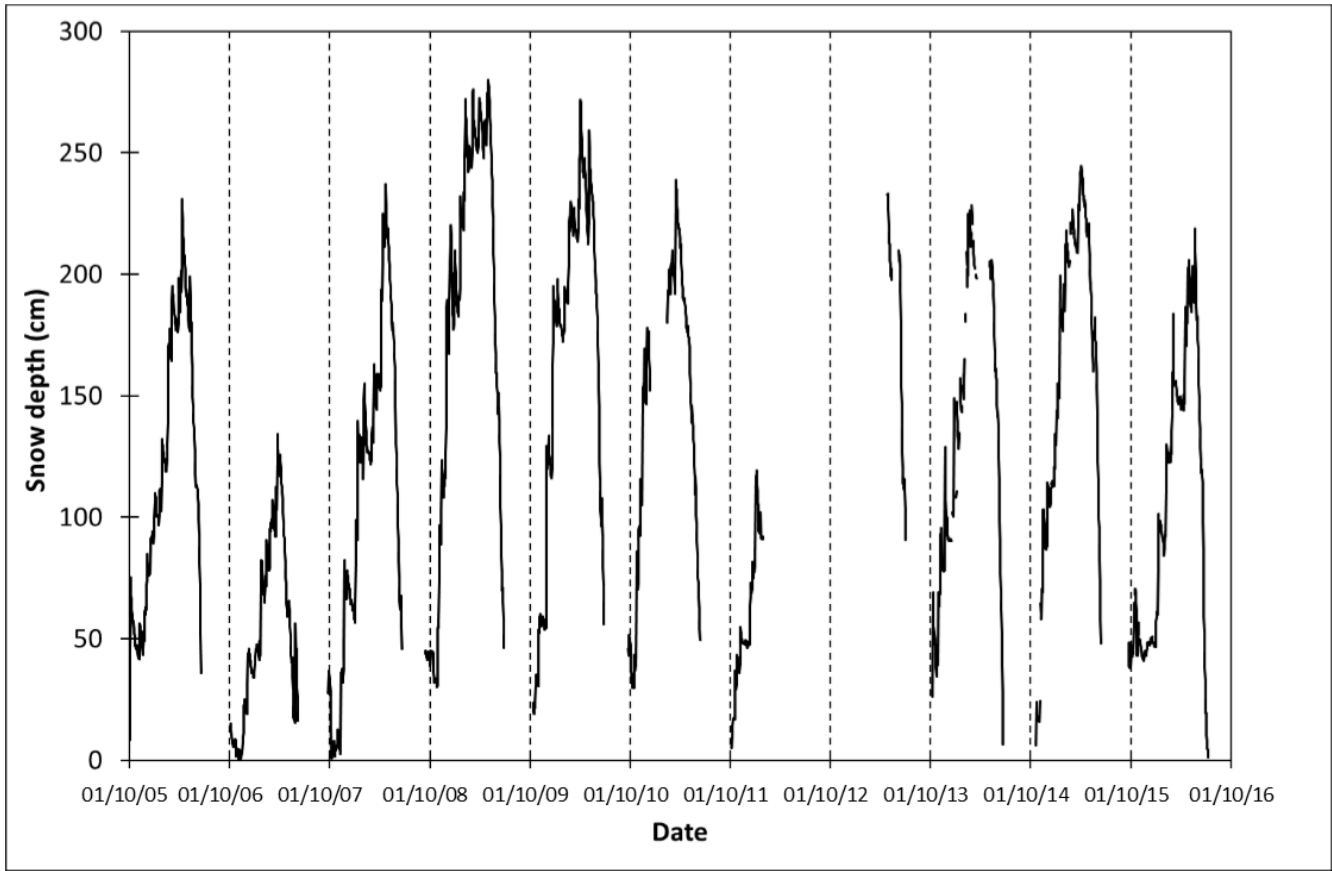
557

558

559

560

Figure 1: (a) The study site. The yellow triangle indicates the location of the AWS1 Forni and the Forni AWS SPICE until November 2015. The red star refers to the actual location after securing the stations. (b) AWS1 Forni (on the right) and AWS Forni SPICE (on the left) photographed from the North-East on 6th May 2014 (immediately after the installation of the AWS Forni SPICE). The distances between the stations are shown.



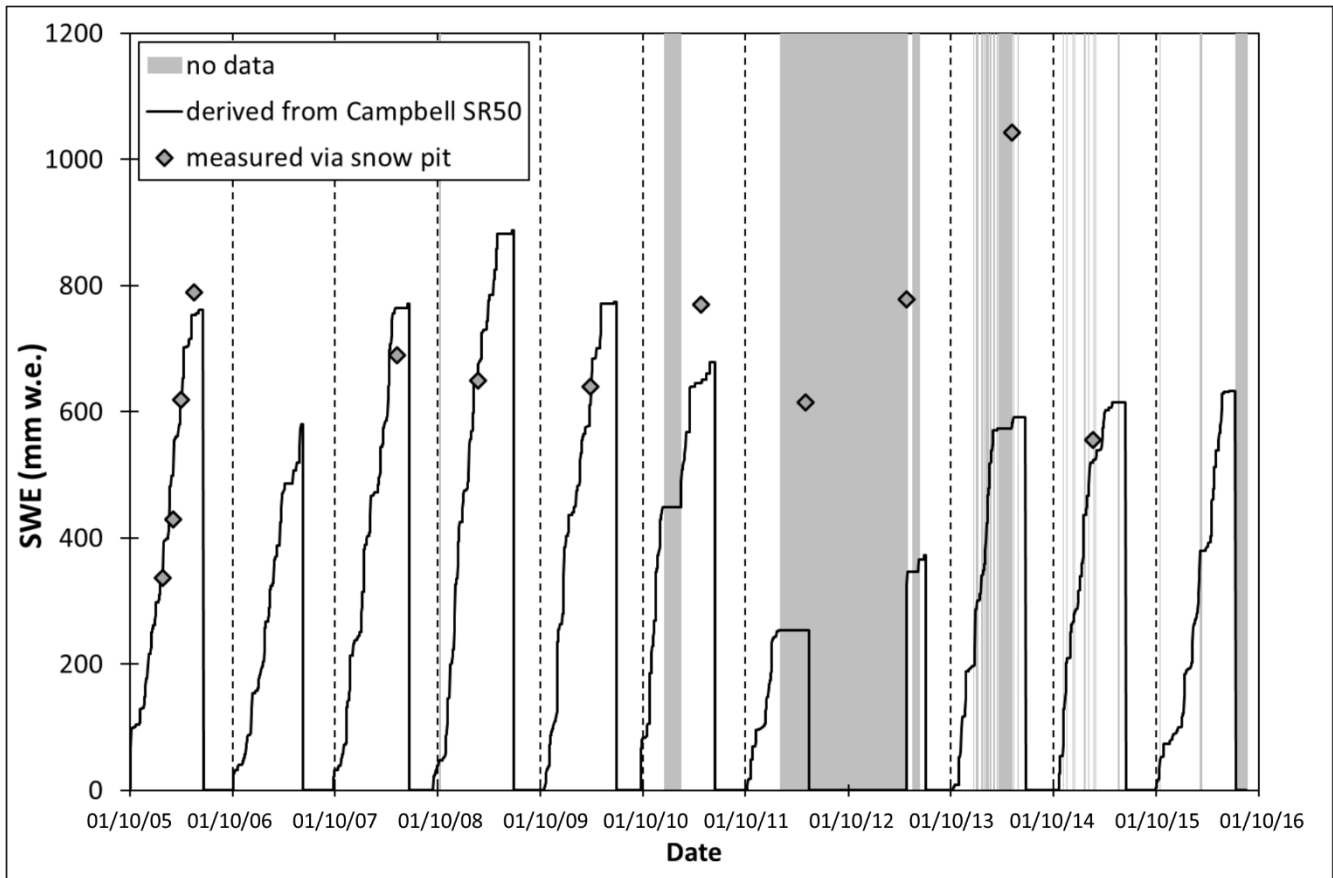
561

562 **Figure 2: Daily snow depth measured by the Campbell SR-50 sonic ranger at the AWS1 Forni from 1st October 2005**

563 **to 30th September 2016. The dates shown are dd/mm/yy.**

564

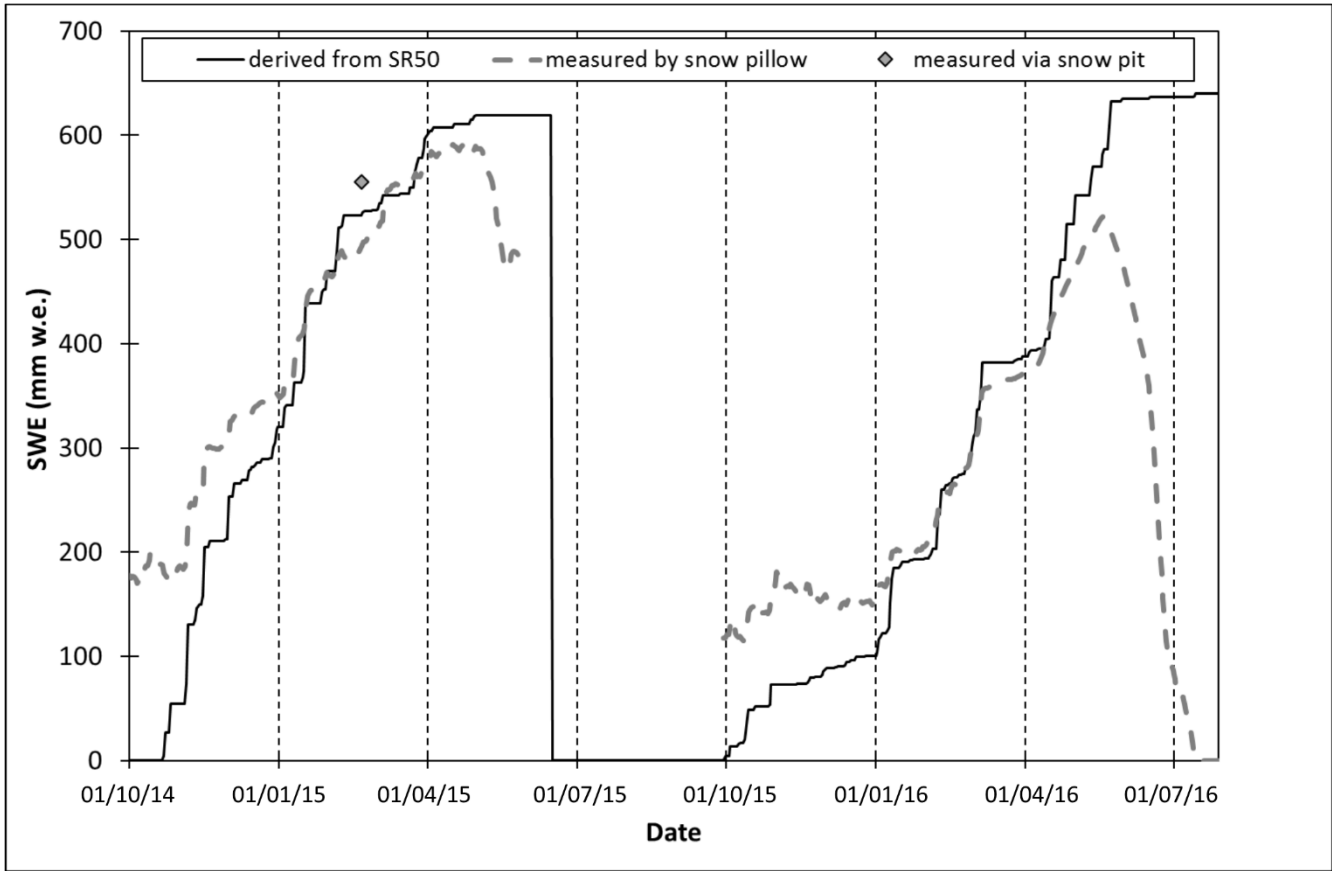
565



566

567 **Figure 3: Daily SWE data derived from snow depth by the Campbell SR50 (using the new snow density of 149 kg m^{-3}) and measured by snow pits from 1st October 2005 to 30th September 2016. The periods without data are shown in**
 568 **light grey. The dates shown are dd/mm/yy.**

570

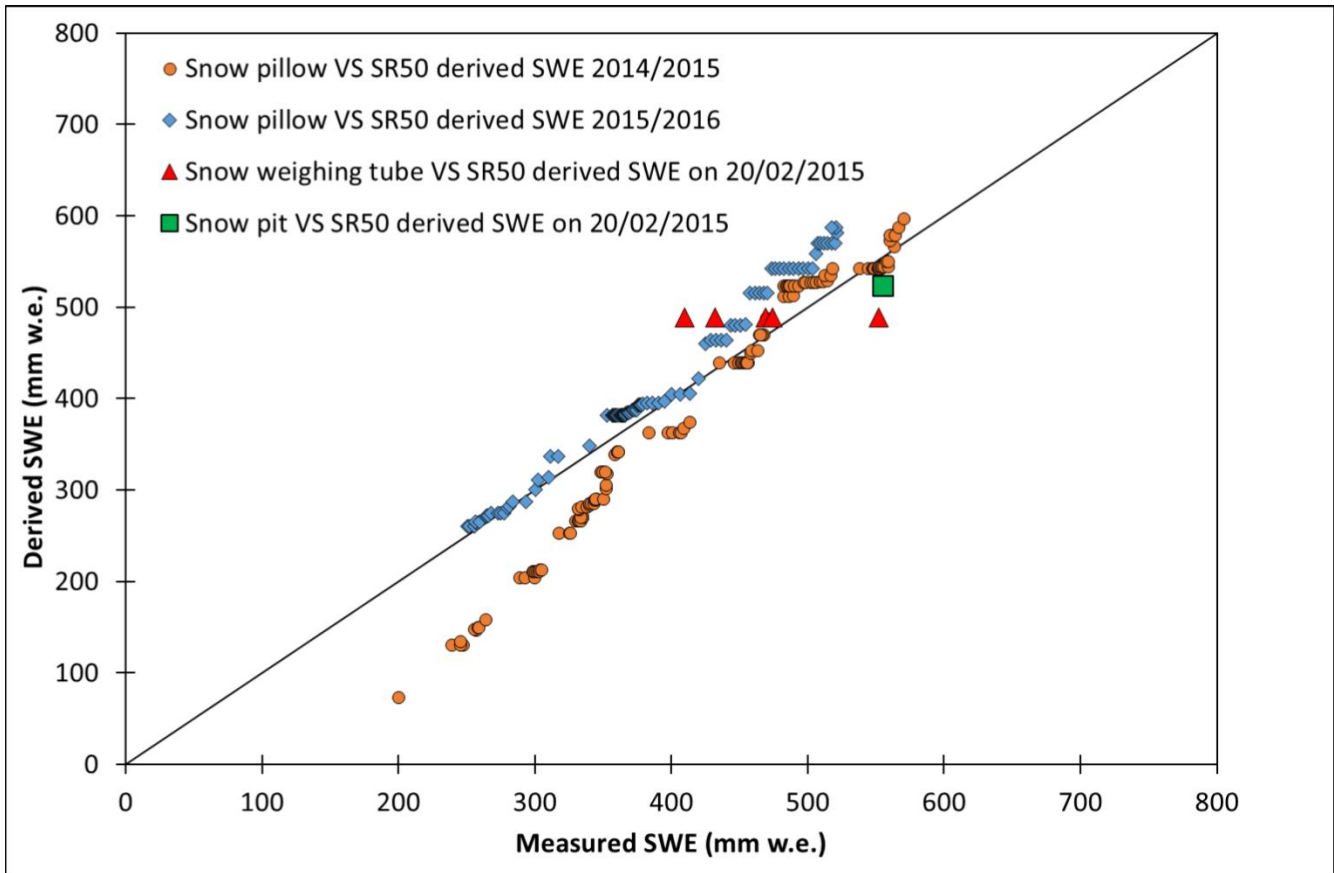


571

572 **Figure 4: Daily SWE data derived from snow depth measured by Campbell SR50 (using the new snow density of 149**

573 **kg m⁻³) and measured by snow pits and snow pillow from October 2014 to July 2016. The dates shown are dd/mm/yy.**

574



575

576

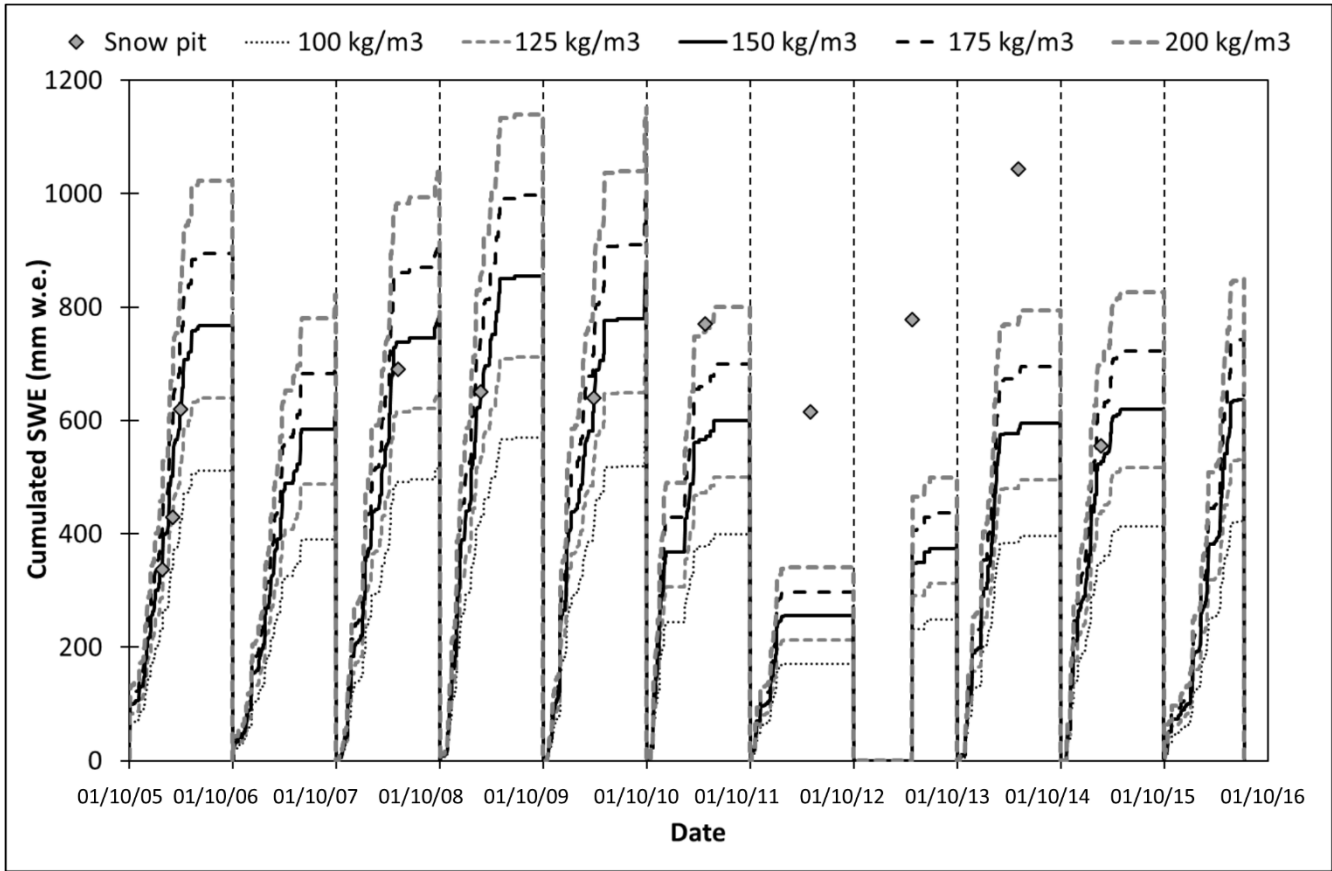
577

578

579

580

Figure 5: Scatter plots showing SWE measured by snow pillow and snow pit and derived applying Eq. (4) to data acquired by Campbell SR50 (using the new snow density of 149 kg m^{-3}). Two accumulation periods of measurements are shown from November 2014 to March 2015 and from February 2016 to May 2016. Every dot represents a daily value.



581
 582 **Figure 6: Comparison among daily SWE values derived from snow depth data acquired by SR50 sonic ranger**
 583 **(applying different values of new snow density) and SWE values measured by snow pits from 2005 to 2016. The dates**
 584 **shown are dd/mm/yy.**
 585